Diffractive lens fabricated with binary features less than 60 nm

Joseph N. Mait

U.S. Army Research Laboratory, AMSRL-SE-E, 2800 Powder Mill Road, Adelphi, Maryland 20783

Axel Scherer and Oliver Dial

Department of Electrical Engineering, California Institute of Technology, Pasadena, California 91125

Dennis W. Prather and Xiang Gao

Department of Electrical Engineering, University of Delaware, Newark, Delaware 19176

Received October 15, 1999

We designed, fabricated, and characterized a binary diffractive lens with features less than 60 nm. The lens was designed for operation in the red portion of the spectrum. Experimental measurements of lens performance agree with predictions generated by rigorous models of diffraction. © 2000 Optical Society of America

OCIS codes: 050.1970, 220.3630, 220.4000, 220.3740, 050.1960.

The transmission and distribution of information from an array of sources to an array of detectors in a free-space optical interconnect requires passive optical elements capable of providing focusing, collimation, fan-out, and fan-in.[1] To keep the system compact requires that the elements be easily integrated with active devices and capable of bending light at large angles, which is more easily achieved with diffractive optics than with refractive optics. However, the diffractive element must have features that are either of the order of the operating wavelength or less, and recent developments in computing and fabrication have made possible the design and fabrication of such elements.[2–11] For example, advances in fabrication have produced grating deflectors with minimum features of the order of 100 nm and 20° deflection angles for 633-nm operating wavelengths.[11]

Cylindrical[9] and circular lenses[10,11] have also been produced that use pillars to area encode the desired phase. Kipfer *et al.*[9] demonstrated the first binary subwavelength lens using 10.6-μm illumination. The structure corresponded to a 20° off-axis cylindrical lens with a 3-cm focal length and a 4-cm aperture ($f/0.75$). The pillar pitch was 7.5 μm, and the smallest pillar width was 1 μm. The lens was fabricated in a silicon dioxide substrate (SiO_2, $n = 1.5$) with an etch depth of 7 μm. Chen and Craighead[10] were the first to demonstrate a binary subwavelength lens operating at 633 nm. The structure corresponded to an on-axis spherical lens with 20-mm focal length and 1-mm aperture ($f/20$). The pillar pitch was 700 nm, and the smallest pillar width was 350 nm. The lens was also fabricated in SiO_2 with an etch depth of 1 μm. More recently, Lalanne *et al.*[11] used 860-nm illumination to demonstrate a 20° off-axis spherical lens with a 400-μm focal length and a 200-μm aperture ($f/0.5$). The pillar pitch was 405 nm, and the smallest pillar width was 120 nm. The lens was fabricated in titanium dioxide (TiO_2, $n = 2.3$) with an etch depth of 990 nm.

Using annular rings instead of pillars to encode phase, we demonstrate a binary subwavelength on-axis spherical lens in the visible spectrum that is smaller and optically faster than the lenses cited above. The lens has a measured 65-μm focal length and a 36-μm aperture ($f/1.75$). The ring pitch is approximately 160 nm, and the minimum ring width is less than 60 nm. The lens was fabricated in SiO_2, with an etch depth of 400 nm. In addition, to validate the performance of the lens, we compare the experimental results with predicted results for a lens with fabrication errors. We briefly describe the lens design, fabrication, and experimental characterization.

To design a diffractive element that realizes a specific wave-front transformation using subwavelength features, one can use an effective refractive index to map the desired superwavelength function onto a subwavelength form. If the superwavelength behavior can be represented as a phase transformation $\theta(x)$, the refractive index associated with it is

$$n_{\mathrm{eff}}(x) = (n_s - n_0)\left[\frac{\theta(x)}{\theta_0}\right] + n_0\,, \tag{1}$$

where

$$\theta_0 = \frac{2\pi d(n_s - n_0)}{\lambda}\,, \tag{2}$$

d is the etch depth of the binary element, n_0 is the refractive index of the medium exterior to the element substrate, and n_s is the refractive index of the element substrate. The phase θ_0 is the maximum phase that the diffractive element can obtain. If the desired phase exceeds θ_0, then $\theta(x)$ must be clipped to a range of phase values equal to θ_0.[12]

0146-9592/00/060381-03$15.00/0

To encode $n_{\mathrm{eff}}(x)$ into a binary subwavelength profile $t(x)$, we use pulse-width modulation,[4,6,9,10,12]

$$t(x) = d \sum_{m=-\infty}^{\infty} \mathrm{rect}\left(\frac{x - m\Delta - g_m\Delta/2}{g_m\Delta}\right), \qquad (3)$$

where $g(x)$ is a function of the effective index $n_{\mathrm{eff}}(x)$ and $g_m = g(m\Delta)$ is its sampled representation. The sampling distance Δ is of the order of λ/n_s. The relationship between $g(x)$ and $n_{\mathrm{eff}}(x)$ can be calculated either with rigorous electromagnetic models or with approximate ones.[13]

Because area is related to phase in our encoding scheme, the change in phase $\theta(x)$ determines the minimum feature δ that is necessary to resolve the phase accurately. However, fabrication technology limits the minimum feature size $\delta_{\min}$ that can actually be realized. If the required feature size δ is less than $\delta_{\min}$, the pattern must be spatially quantized.[12]

Using this procedure, we designed an axisymmetric 100-μm focal-length, 45-μm-diameter binary subwavelength diffractive lens. The lens was designed to have a 60-nm minimum feature and to operate with 600-nm illumination. The design etch depth was 600 nm, which yields a feature aspect ratio of 10:1. To achieve a larger aspect ratio would have required either a smaller minimum width, which we felt we could not reliably achieve, or a deeper etch, which would have presented mechanical stability problems for the electron-beam resist used in fabrication.

Unlike previous lens designs, which encoded the phase by use of subwavelength pillars,[10,11] we encoded the phase by use of subwavelength annular rings. To do so, we accounted for the annular nature of our structures in the area calculations that relate $g(x)$ to $n_{\mathrm{eff}}(x)$ in Eq. (3). A radial cross section of the lens is represented in Fig. 1. The 2π-continuous-phase function represents our desired lens phase $\theta(x)$. The phase-limited function results after we account for the 600-nm etch depth and represents the phase that we encoded according to Eq. (3).

The lens was fabricated by use of electron-beam lithography to define the 60-nm minimum feature. The SiO_2 substrate was patterned with a gold mask. To improve gold adhesion to the substrate, we sputtered a 20-nm surface layer of silicon nitride onto the substrate first. This was followed by a thermally evaporated 150-nm layer of gold. A 70-nm layer of the electron-beam resist poly(methyl methacrylate) (PMMA) was spin coated above the gold layer.

We used electron-beam writing to pattern the PMMA, using a Hitachi S-4500 scanning electron microscope with a 30-kV acceleration voltage. Following exposure, the PMMA was developed in a 3:7 concentration of 2-ethoxyethanol and methanol. We then performed ion milling with argon gas to remove the gold in the areas where the PMMA was exposed. Gold is etched by this ion bombardment at four times the rate of PMMA.

Once the pattern was transferred to the gold layer, we applied reactive-ion etching to the substrate. The etching process employed an $Ar-Cr_2F_6$ gas mixture at a pressure of 20 mTorr, with a flow rate of 4 SCCM (SCCM denotes cubic centimeters per minute at STP) for Ar and 10 SCCM for C_2F_6. The plasma was maintained with 50 W of high-frequency power, which produced a bias voltage of -360 V. Figure 2 is a picture of the etched lens taken with a scanning electron microscope. The design profile is provided for comparison. Note that all features in the desired profile are visible in the etched lens.

We characterized the physical attributes of the lens, using a Wyko white-light interferometer. The measured diameter was 36 μm, and the measured etch depth was 400 nm. Although we were unable to measure the size of the minimum feature, if we assume that the 80% scaling from the 45-μm design diameter to the 36-μm measured diameter can be applied to the entire structure, the minimum feature is of the order of 48 nm. The errors in lateral scale and depth are due to errors in the calibration of the pattern writing and etch processes, which we are still refining.

Nonetheless, the recent development of tools to analyze rigorously diffractive elements with subwavelength structures[14] allowed us to verify the

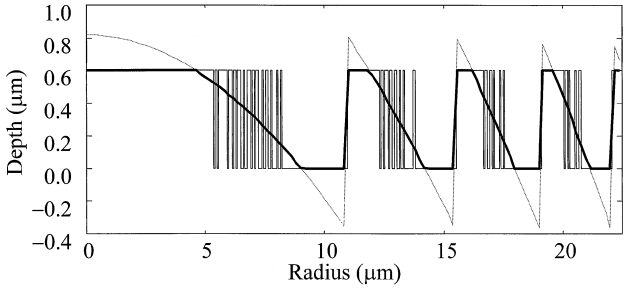

Fig. 1. Depth profile of axisymmetric binary subwavelength lens in radial cross section. 2π-continuous-phase lens and limited-phase lenses used to obtain the binary profile (dashed line) are also shown (heavy solid line).

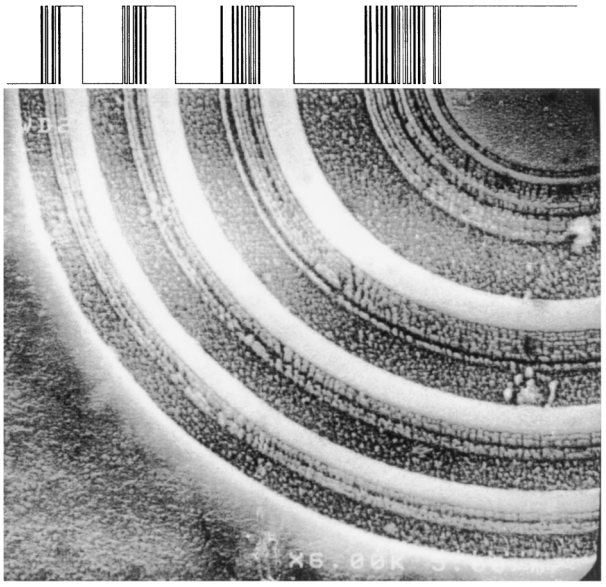

Fig. 2. Etched subwavelength lens taken by scanning electron microscope. The desired binary profile is shown for comparison.

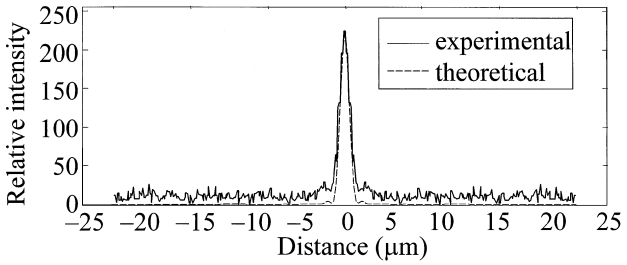

Fig. 3. Line scans of simulated and experimentally measured intensity responses at a plane 65 μm from lens.

performance of the fabricated element as a lens. (The presence of subwavelength features invalidates a scalar-based analysis of the lens.) We used the measured parameters to scale our design profile and analyze the subsequent structure with a finite-difference time-domain technique for rotationally symmetric structures.[14] The analysis predicted a 65-μm focal length, which we verified experimentally.

Figure 3 is a comparison between the measured response of the lens at the plane 65 μm from the lens and the response predicted by the analysis. Note that, neglecting noise and bias, the basic shape of both responses is similar. The width of the central lobe, taken as the width between the first two minima, is approximately 3 μm for both lenses. Further, even in the presence of noise, the sidelobes exhibited in the experimental results line up with the predicted sidelobes. The noise and the bias in the experimental response were generated by the low-dynamic-range 8-bit detector, which effectively has only 5 bits of dynamic range; the noise floor of the detector is at the third bit.

Although other groups[9–11] have reported fabrication of subwavelength lenses, the lenses were larger, had larger feature sizes, and provided no analysis of their lens structures. Our analysis capabilities in combination with optical characterization allowed us to account for fabrication errors and to confirm the observed experimental behavior with simulations. Further refinement of our fabrication and characterization procedures is planned, as well as a more-detailed characterization of lens performance.

J. Mait's e-mail address is mait@arl.mil.

References

1. H. Martinsson, J. Bengtsson, M. Ghisoni, and A. Larsson, IEEE Photon. Technol. Lett. **11,** 503 (1999).
2. Z. Zhou and T. J. Drabik, J. Opt. Soc. Am. A **12,** 1104 (1995).
3. F. T. Chen and H. G. Craighead, Opt. Lett. **20,** 121 (1995).
4. M. E. Warren, R. E. Smith, G. A. Vawter, and J. R. Wendt, Opt. Lett. **20,** 1441 (1995).
5. R. E. Smith, M. E. Warren, J. R. Wendt, and G. A. Vawter, Opt. Lett. **21,** 1201 (1996).
6. J. M. Miller, N. de Beaucoudrey, P. Chavel, E. Cambril, and H. Launois, Opt. Lett. **21,** 1399 (1996).
7. S. Astilean, Ph. Lalanne, P. Chavel, E. Cambril, and H. Launois, Opt. Lett. **23,** 552 (1998).
8. Ph. Lalanne, S. Astilean, P. Chavel, E. Cambril, and H. Launois, Opt. Lett. **23,** 1081 (1998).
9. P. Kipfer, M. Collischon, H. Haidner, J. T. Sheridan, J. Schwider, N. Streibl, and J. Lindolf, Opt. Eng. **33,** 79 (1994).
10. F. T. Chen and H. G. Craighead, Opt. Lett. **21,** 177 (1996).
11. Ph. Lalanne, S. Astilean, P. Chavel, E. Cambril, and H. Launois, J. Opt. Soc. Am. A **16,** 1143 (1999).
12. J. N. Mait, D. W. Prather, and M. S. Mirotznik, Opt. Lett. **23,** 1343 (1998).
13. J. N. Mait, D. W. Prather, Ph. Lalanne, and M. Collischon, in *Diffractive Optics*, Vol. 22 of European Optical Society Topical Meetings Digest Series (European Optical Society, Jena, Germany, 1999), pp. 32–33.
14. D. W. Prather and S. Shi, J. Opt. Soc. Am. A **16,** 1131 (1999).